International Journal of Smart Home
Vol. 10, No. 7 (2016), pp. 291-300
http://dx.doi.org/10.14257/ijsh.2016.10.7.29

Research on Antenna Arraying Combining Technology for Deep Space Measurement & Control

Ke Sun and Xiaomin Hou

Equipment Academy, Beijing 101416, China
sk2220060710@126.com

Abstract

In this dissertation, the key technology of uplink array for deep space TTC is studied. Based on the concept of power combining, the theoretical analysis is made on the uplink array. The spatial power combining can be achieved in a certain power. The uplink antenna array technology is a power combiner. At first this chapter introduces the principle of power combining and leads to the concept of the uplink antenna arraying. Then analyze the theory of the uplink antenna arraying power combining, including the signal strength and antenna pattern. The influence of the number of element, spacing, phase and time delay on power combining is analyzed by simulation. At last the uplink antenna arraying power combining performance is analyzed and verified by simulation.

Keywords: *power combining; uplink antenna arraying; the signal strength; antenna pattern; time delay*

1. Introduction

In deep space exploration, the signal transmitting between spacecrafts and ground stations is faced with huge path loss, and the high performance of ground antennas (EIRP and G/T) are required. Uplink antenna arraying is a potential technique used for deep space tracking and telecommunication that have many advantages such as low cost, high performance and flexibility. It can not only raise the communication data rate, provide longer operation distance, but also make future mission have lower cost and more flexible design. With the depth of theoretical research, foreign country conducts several experiments of uplink antenna arraying. These experiments use different caliber antennas to verify different methods of phase calibration. Error factors affecting phase calibration is used to test and research. Successful experiments are laying the foundation for further practical application.

Since 2006 NASA's JPL used the 34m antenna beam waveguide of the Goldstone Deep Space Network and Conducted several experiments of the uplink antenna arraying. The experiments are carried out in chronological order. In February 25, 2006, the JPL conducted the first experimental demonstration of the uplink antenna arraying using two 34m beam waveguide antennas (Apollo deep space station of DSS-24 and DSS-25) in the Goldstone Deep Space Communications Station under the real operating environment [1]. The experimental principle is shown in Fig. 1.

In 2007 JPL's V. Vilnrotter *et al* did the far field experiments of the uplink antennas arraying using Moon-bounce algorithm to verify the feasibility of uplink arraying carrier phase calibration [2][3]. Transmit the uplink signals as a natural reflection of the far field source using three 34m beam waveguide antennas (DSS-24, 25, 26). Wherein, Moon-bounce algorithm is a calibration method using RDDI (Radar Doppler Delay Imaging) technique for phase correction.

In June 27, 2008, V. Vilnrotter *et al* used three 34m antennas tracking EPOXI spacecraft in the uplink antenna arraying experiments at Goldstone [4][5]. In the experiment

ISSN: 1975-4094 IJSH

three antennas transmitted remote control signal whose carrier is the X-band of 7.2GHz. The elevation angle ranges of the antennas are 30°-60°. And the high-gain antennas of EPOXI spacecraft are pointed towards to planet Earth.

In 2005 Larry D'Addario began to use the method of phase calibration and discussed the feasibility of this method. Between 2007 and 2008 through the program of demonstration and test platform, they did the small-scale and small-diameter experimental verification of uplink antenna arraying [6].

In 2010 Dr. Xueshu Shi studied the calibration methods of uplink arraying in equipment academy [7]. The method of phase correction based on the principles of the Moon-Bounce phase correction (DRAD: Phase Ramp Amplitude Difference) is proposed. The method is used to measure the phase difference among the antennas depending on the exact position and the geometry of the antenna elements and observation pixel as well as the variation of imaging interference fringes.

This paper describes the research background of the uplink antenna arraying and analyzes the advantages and difficulties of the uplink antenna arraying. Clarify the important role of the uplink antenna arraying in the future development of space technology. Analyze several ongoing trials and Achievements for uplink arraying.

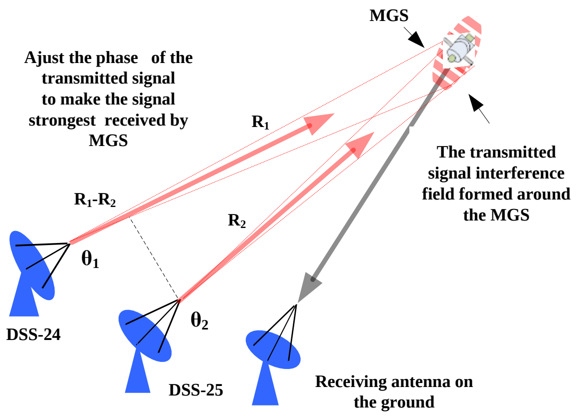

Figure 1. The Experimental Principle of the Uplink Arraying based on the Detector MGS

2. The Analysis of the Uplink Antenna Arraying Combining Power Factors

2.1. Analysis of the Signal Strength

At first, we assume the situation that two binary array antenna transmit the pure sinusoidal signal. As long as all the contents of the modulation signal antennas are consistent and aligned with each other in reaching the targe. Then the signal is the same as the result of the sinusoidal modulation. The signal form and polarization of Two yuan arrays is the same as a sinusoidal signal. The strength $E(t)$ of the far-field synthesis signal at the target can be expressed as:

$$E(t) = e_1 \cos(2\pi ft + \phi_1) + e_2 \cos(2\pi ft + \phi_2) \quad (1)$$

Wherein: e_1, e_2 represents the electric field strength of the two transmit antennas signals. f represents the signal of the carrier frequency, ϕ_1, ϕ_2 represents the carrier phase. Analyze the impact of carrier phase difference. It is assumed that $e_1 = e_2 = e$. At this time the equation becomes:

$$E(t) = e\left[\cos\left(2\pi ft + \phi_1\right) + \cos\left(2\pi ft + \phi_2\right)\right] \quad (2)$$

When $\phi_1 = \phi_2$, phase difference between two signals is zero. The signal is the coherent superposition. The amplitude of the received signal is twice of the single signals at the target. It is four times of the power of the single signal. When $\phi_1 = \phi_2 + \pi$, the phase difference of two signals is π. The strength of the received signal is $E(t) = 0$ at the target. The phase relationship between the signal of each element and the synthesis of strength is closely. The far field power density P of two antennas synthesized can be expressed by the following formula:

$$\begin{aligned} P &= \langle E(t)^2 \rangle / Z_0 \\ &= \left(\mathrm{e}^2 / Z_0\right)\left[2 + 2\left\langle \cos\left(2\pi ft + \phi_1\right)\cos\left(2\pi ft + \phi_2\right)\right\rangle\right] \\ &= \left(\mathrm{e}^2 / Z_0\right)\left[2 + 2\cos\left(\phi_1 - \phi_2\right)\right] \\ &= 2P_0\left[1 + \cos\left(\phi_1 - \phi_2\right)\right] \end{aligned} \quad (3)$$

Wherein: Z_0 represents the intrinsic impedance of free space. P_0 represents a single antenna far-field power of the transmitted signal which is $P_0 = \mathrm{e}^2 / Z_0$. $\langle \ \rangle$ represents the average access time. When the phase difference of the two antenna-carrier is zero, the synthesis of both the power density can be maximized, namely:

$$P_{\max} = 4P_0 \quad (4)$$

Therefore, it can be concluded: the strength of binary arrays field is up to four times the power of a single antenna. When the numbers of uplink antenna arrays are set, in the general case the far field signal strength is such as.

$$E(\mathrm{t}) = \sum_{i=1}^{N} e_i \cos\left(2\pi ft + \phi_i\right) \quad (5)$$

Wherein: e_i , ϕ_i represents respectively the signal strength and the carrier phase of transmitted signal of the i antenna. Suppose $e_i = e$, the far field power density P at the same target is expressed as:

$$\begin{aligned} P &= \langle E(t)^2 \rangle / Z_0 \\ &= \left(\mathrm{e}^2 / Z_0\right)\left\langle \sum_{i=1}^{N}\cos^2\left(2\pi ft + \phi_i\right) + \sum_{i=1}^{N}\sum_{j=1, i\neq j}^{N}\cos\left(2\pi ft + \phi_i\right)\cos\left(2\pi ft + \phi_j\right)\right\rangle \\ &= \left(\mathrm{e}^2 / Z_0\right)\left[\frac{N}{2} + \frac{1}{2}\sum_{i=1}^{N}\sum_{j=1, i\neq j}^{N}\cos\left(\phi_i - \phi_j\right)\right] \\ &= P_0\left[N + \sum_{i=1}^{N}\sum_{j=1, i\neq j}^{N}\cos\left(\phi_i - \phi_j\right)\right] \end{aligned} \quad (6)$$

If the carrier phases of transmitted signals of all the antennas are aligned that is $\phi_i = \varphi$, the maximum of power density is:

$$P_{max} = [N + (N-1)N]P_0 = N^2 P_0 \tag{7}$$

It can be seen that N element antenna uplink array can achieve far field power density relative to a single antenna.

2.2 Analysis of the Antenna Pattern

For the purposes of antenna aperture, its value of far-field radiation can be calculated by the equivalence principle. Based on the principle of equivalence, when any field source is inside any closed surface S_0, external field intensity distribution at any point can be uniquely determined by the components of the electromagnetic field S_0 on the tangential surface[8] In addition to use the equivalent source methods, the fourier transform method can be used to calculate. The far field distribution of the antenna is equal to fourier transform of near-field distribution[9]. By solving the antenna aperture field to calculate the far field radiation field, improve the calculation accuracy of the main lobe and the paraxial sidelobes by the means of the method. If the amplitude and phase of the circular aperture antenna field is uniform, the antenna is a uniform circular aperture antenna. If the electric field the caliber is along the y direction of polarization, the far radiation field M of the single antenna from the radiation integral formula [10].

$$E_M = j\frac{(1+\cos\theta)\pi E_0 e^{-jkr}}{2\lambda r}\cdot\frac{a^2 J_1(ka\sin\theta)}{ka\sin\theta} \tag{8}$$

Wherein: θ is the angle between the connection of the origin to M point with the antenna axis. E_0 is the amplitude of the center antenna aperture plane. k is the beam and λ is the wavelength, $k=\frac{2\pi}{\lambda}$. r is the Distance which is the center of the antenna to far field M . a is the radius of the antenna aperture surface. $J_1(\cdot)$ is the first class of first-order Bessel function. Port size is usually much larger than the wavelength, radiation field energy is concentrated within a small angular range θ . $\cos\theta$ is a slowly varying function. The direction characteristic of the antennas can not be considered. The formula is normalized to achieve a single antenna function is as follows.

$$F(\theta) = \frac{2J_1(ka\sin\theta)}{ka\sin\theta} \tag{9}$$

If the phase of the power field is uniform, the maximum radiation direction of the main lobe is along the normal axis direction of $\theta = 0°$. Due to the power distribution field is rotationally symmetric, the function of the normalization direction is also rotational symmetry. The Figure 2. shows the far field pattern that a 34m single antenna from the Earth to the Moon [11].

Similarly, in terms of the binary antenna array, it's far field distribution is fourier transform of arraying far-field. Binary arrays can be seen as a normalized function of antenna and the convolution which is located in the two antenna phase center. Fourier transform domain will lead to far-field distribution of the antenna signal and sinusoidal interference pattern. It is similar to Young's double slit interference principle. The Figure 3. is the two 34m antenna far-field interference pattern under the same conditions. The far field pattern of the antenna array forms a clear interference fringes where is the coherent superposition of the signal at the center. The radiation intensity is twice the single antenna. Combining power is four times the single antenna. Since the radiation power is reduced to zero in the far-field region of the two signal carrier phase., it is related to carrier signal phase alignment of each antenna in a certain direction. Conversely, you can adjust the value size of the combining power in the direction by changing the phase difference between the antennas.

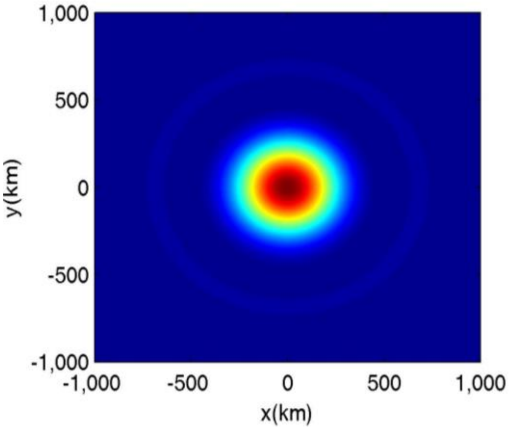

Figure 2. The Far Field Pattern of a Single 34m Antenna

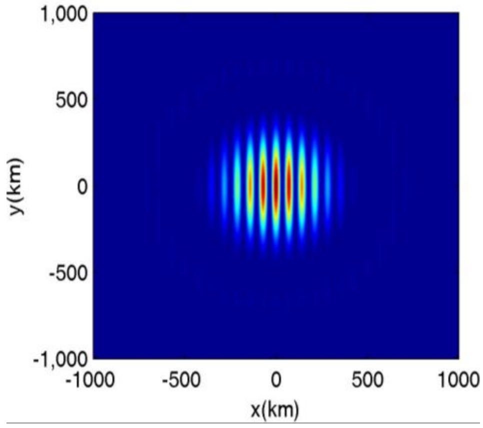

Figure 3. The Far Field Pattern of Binary 34m Arrays

3. Preliminary Analysis of the Uplink Antenna Arraying Power Combining Performance

Based on the above analysis, the uplink antenna arraying can effectively increase the transmitted signal power. Use matlab to simulate for far-field power combining performance in this section. Analyze the effect of arraying power combining about the number of the array element, array element spacing, the phase difference between array elements and other factors[12]. Wherein, the 34m antenna is relatively symmetrical to the origin. The working frequency is $f = 8GHz$. The lunar distance of $z_1 = 38$ million meters is the far field goal point. Observe the changes of interference fringes in a certain area.

3.1 Effect of Array Elements for Power Combining

As shown in figure 4 (a) and (b) when antenna spacing is $d = 100m$, the far field interference fringes will become narrower from binary arrays from binary arrays to four yuan arrays. However, the number of stripes is not changed and the fringe interval remains unchanged. Analyze and compare figure 4 (c) and (d). It obeys the same rule when the antenna is 200m interval.

It can be concluded that the interference fringes of the arraying far field will be narrow, combining power of center will increase and the number of stripes and the spacing will remain the same when the number of array elements is increasing.

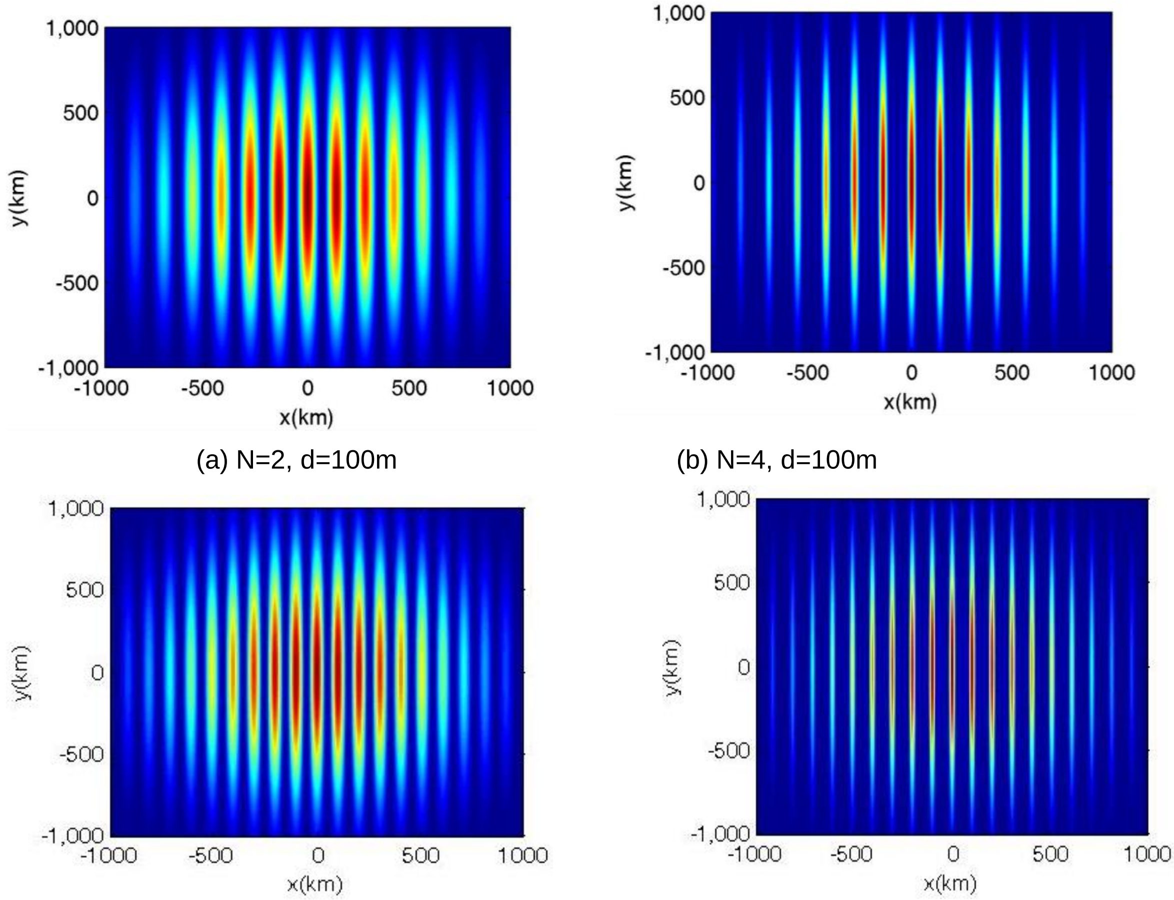

(a) N=2, d=100m

(b) N=4, d=100m

(c) N=2, d=200m

(d) N=4, d=200m

Figure 4. The Effect of Array Elements and the Spacing on the Far Field Pattern

By comparing with Figure 4 (a) and (c), interval of binary arrays is increased from 100m to at 200m. In the same region, the the number of interference fringes of the far-field is increased and the striped distribution is more intensive. But the width of a single stripe is narrowed, the relative distance between the two fringes decreases. By comparing with Figure 4 (b) and (d), It can be also concluded that the array element spacing is increased, the number of stripes is increased, the spacing is decreased and the width is narrow for four yuan arrays. The simulation calculation shows that the power combining gain of the center will be decreased.

3.2 The Impact of Power Combining caused by Phase

Maximum power combining value will be achieved for binary array when the carrier phases of the two signals are aligned at the target point for binary array. Assume the space $d = 200m$ of the binary array which is satisfied with symmetrical distribution. The phase difference generated by the distance is zero. Analyze power combining affected by phase. In the experiment the left side of the antennas is maintained to be the same phase. Only adjust the initial phase of the right side of the antennas. Simulate the interference fringes of the target area which is changed when the phase difference $\Delta\phi$ of the two antennas is respectively 0°, 45°, 90° and 180°. Wherein the field of observation is in the range of 300 km. The far field value of each point is normalized. Observe the size of the center point.

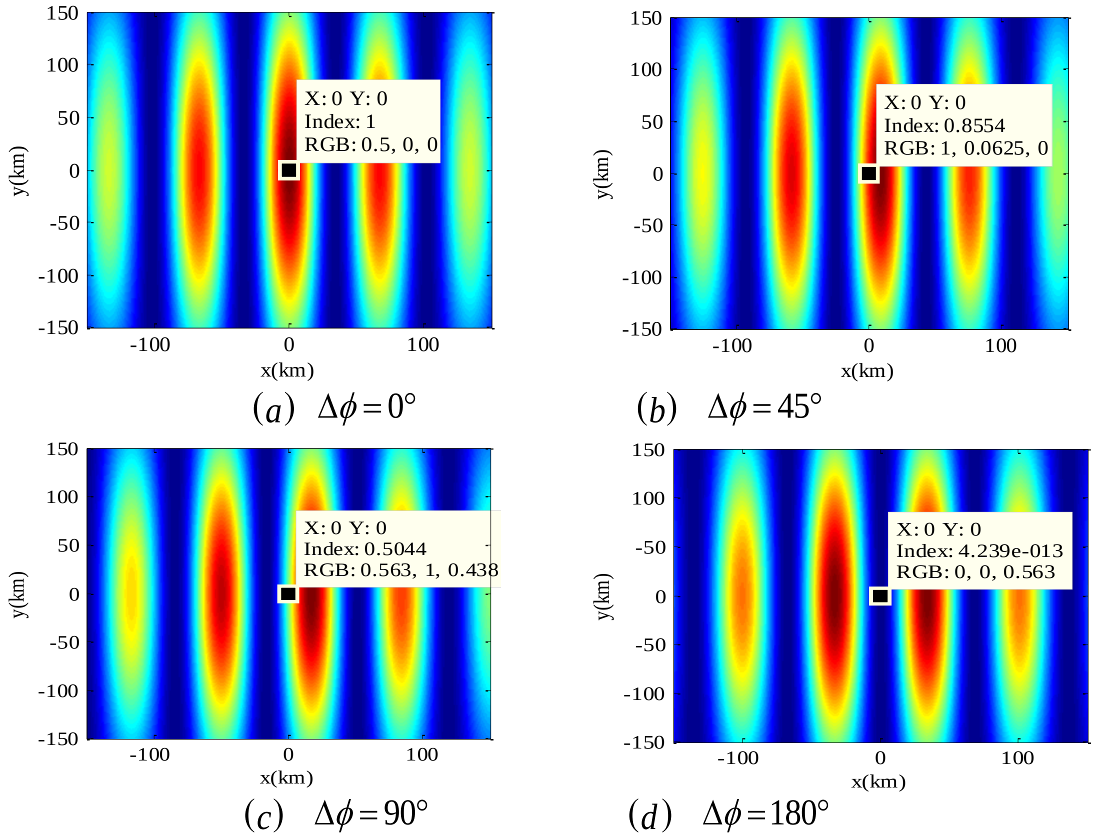

Figure 5. The Far Field Pattern Effected by Different Phase Difference

The results of simulation are shown in figure 5. It can be seen that the peak power point moves gradually to the right from the analysis and comparison of four graphs. And the peak size will gradually be decreased. The normalized value of maximum peak power when the phase difference is 0°. The received power of the center is reduced to 0 when the phase difference is increased to 180°. At this time two signals are interfered with cancellation. It is reflected that the impact of the carrier phase difference of array element is changed by arraying power combining. By observing the interference fringes in practice, Adjust the signal phase of antennas appropriately. In order to achieve the purpose of compensate phase difference, make the value of uplink antenna arraying combining power maximum.

3.3 The Impact of Power Combining caused by Delay

When the carrier phases of the two signals are perfectly aligned, the value of power combining is affected by the delay difference between the two signals. Firstly, assume the ratios between the symbol width of the signal and delay difference of the signal is N. Then assume the spacing of two antennas is D and the distance difference of the two uplink signals reaching the same goal in deep space is d. The direction between the signal transmission and the antenna connection is in the same plane. Finally the angle is θ [13]. As shown in Fig. 6.

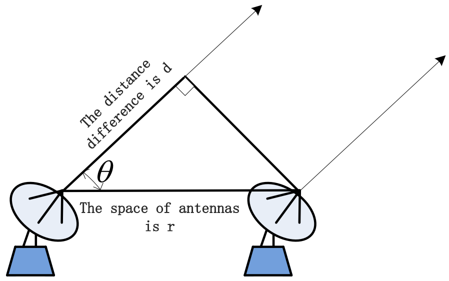

Figure 6. The Relations of the Geometric Delay Difference and the Spacing of the Antennas and the Signal Direction

Fig. 6 reflects the relations of the geometric delay difference and the spacing of the antennas and the signal direction at the target. The distance difference $d = D\cos\theta$ of two uplink signal reaching the target. The delay difference is the ratio of the distance difference and the speed, namely $\tau = \frac{D\cos\theta}{c}$. Wherein c is the speed of light. The symbol rate R_s is assumed. In the excitation source do not adjust symbol delay of transmit signal. The loss of combining power caused by the delay difference is maintained at an acceptable range When N=10. The time delay difference of two uplink signals reaching the target is less than or equal to the 1/10 width of the signal symbol [14].

$$\frac{D\cos\theta}{c} < \frac{1}{10R_s} \tag{9}$$

That is,

$$R_s < \frac{c}{10D\cos\theta} \tag{10}$$

According to the formula, suppose the distance between antennas to be $D = 1km$. Minimum angle of target pitch is $\theta = 10°$. The symbol rate R_s which should be less than 30.462ksps can be obtained into the above formula. If the symbol rate > 30.462ksps, the loss of the signal combining power because of delay difference is in the acceptable range. By changing the phase control word of the DDS achieve the phase shift at the intermediate frequency (excitation source). IF digital phase shift can be easily used to achieve the phase adjustment of the RF signal and the subcarrier signal, as well as time delay adjustment of modulation data. Through the program of the IF digital phase shift, achieve high accuracy of phase adjustment easily. The accuracy is controlled by the width of phase word. The phase adjustment precision of 14bit phase control word is nearly 0.022°. Regardless of the carrier signal, the subcarrier signal or a data symbol, achieve the purpose of improving the accuracy of the phase adjustment by Increasing the width of the phase control word. Thus, in the current technical conditions, achieve by the method of phase IF digital shift to adjust the symbol delay. In practice, compared to the phase adjustment, the time delay adjustment is a lot easier. So the impact on the uplink combining arraying can be ignored.

4. The Calibration and Error Analysis of the Carrier Phase

In the process of carrier phase calibration for uplink antenna arraying system, you need to determine the mutual positional relationship in advance among the terrestrial antenna arraying, calibration target at the receiver, as well as deep space spacecraft. In the process of the calibration, phase difference and carrier phase compensation is obtained by calculating the difference of the geometric distance of the different transmit signals. After the completion of phase calibration, continue to work for long hours to set array beam. If the error of the spacecraft orbit prediction exists, it will bring a new phase error to reduce combining efficiency. Location information error of the entire operating system should be filled with attention. In the Theoretical analysis, the radiated signal is as the center of a certain point which is called the phase center of the antennas. But in fact there is no such a point which can be represented by the area. Namely that the phase center of the antennas is occurred to jitter in this region. In addition, in different directions for antenna radiation, there is still some difference of phase center.

In accordance with geometry of the error distribution established based on figure 7, the number of the element arrays is 6 × 6. Wherein the diameter of antennas is 12m and the spacing of elements is 100m. Analyze the impact of combining power, when the phase center coordinates of elements are uniformly distributed. Measure the value of the loss of combining gain with the respect to the exact coordinates by 100 Monte-Carlo simulation.

From the figure, the effect of the position error of the phase center on the phase calibration is small. Even though the phase center error of the antennas is 6m, the loss of the combining gain introduced is less than 0.2dB. Under the current technical conditions, the measurement of the phase center is nearly centimeter. So the impact of the position error on the uplink antenna arraying system can be ignored.

If the calibration receiver is in the ground, get the exact position of both by geodesy. The accuracy of the location can reach the order of mm. Its impact on the phase error can be ignored. It can be determined that the calibration of satellite antenna is located near field or far field according to the orbital altitude of the satellite and the layout size of the antenna array.

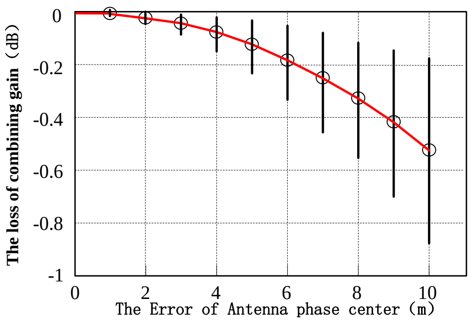

Figure 7. The Relations between the Loss of Combining Gains and the Error of the Phase Center Position

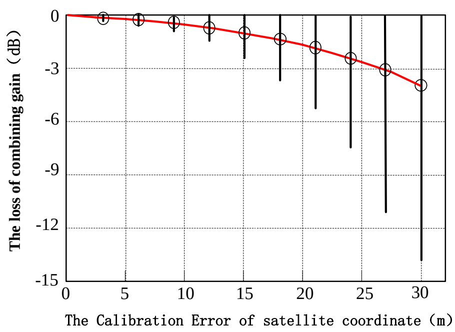

Figure 8. The Relations between the Loss of Combining Gains and the Calibration Error of the Satellite Coordinate

Take advantage of the geometry of the error distribution and maintain the value of each parameter unchanged. Suppose the position coordinates of each array element and deep-space spacecraft precisely known. When the calibration of satellite coordinates is uniformly distributed, simulate the effect on the loss of combining power gain as shown in figure 8.

The impact of the position error of the calibration satellite on the power combining is non-negligible. When the satellites are used for calibration phase, require to install the SLR and GPS systems in the satellite to improve the accuracy of the orbit determination. Reduce the phase error due to satellite position error. Based on the current technology of the satellite orbit determination, the accuracy of the orbit determination in the foreign research institutions (such as CSR, GSFC and JPL) is nearly centimeter [73].

5. Conclusions

Analyze the advantages and difficulties of uplink antenna arraying technology. Clarify the important role of the uplink antenna arraying in the future development of space technology. The primary purpose of the uplink antenna array is set to improve uplink transmission power. The performance of the uplink power combining arraying will be affected by different floor layout of all the antennas. Consider the various constraint conditions of the layout ground and the requirements of the maximum spacing an in entire arraying layout. Multiple antennas simultaneously transmit signals to deep space spacecraft. Analyze the error sources which affect the carrier phase calibration of the uplink arraying, including the measurement of the phase, the calibration error and the phase shift error of the upstream channel. The phase error of the uplink antenna arraying can be controlled within reasonable limit to meet the task requirements. This paper introduces the research background of the uplink antenna arraying. Currently the feasibility of this technique has been verified. It is provided with considerable prospects for development.

References

[1] V. Vilnrotter and D. Lee. Uplink Arraying Experiment with the Mars Global Surveyor Spacecraft [R]. The Interplanetary Network Progress Report, vol. 42-166, Jet Propulsion Laboratory, Pasadena, California, pp. 1–14, August 15, **(2006)**.
[2] V. Vilnrotter, D. Lee, R. Mukai, *et al*. Doppler-Delay Calibration of Uplink Arrays via Far-Field Moon-Bounce Power Maximization [C] Proceedings of the 11th International Space Conference of Pacific Basin Societies (ISCOPS) Conference, Beijing, China, May 15, **(2007)**.
[3] V. Vilnrotter, D. Lee, R. Mukai, *et al*. Three-Antenna Doppler-Delay Imaging of the Crater Tycho for Uplink Array Calibration Applications [R]. The Interplanetary Network Progress Report, vol. 42-169, Jet Propulsion Laboratory, Pasadena, California, pp. 1–17, May 15, **(2007)**.
[4] V. Vilnrotter, P. Tsao, D. Lee, *et al*. EPOXI Uplink Array Experiment of June 27, 2008 [R], JPL IPN Progress Report 42-174E, **(2008)**.
[5] V. Vilnrotter, D. Lee, T. Cornish, *et al*. Uplink Array Concept Demonstration with the EPOXI Spacecreft [J]. IEEEAC paper #1561, Version 4, Updated January 6, **(2009)**.
[6] Larry D'Addario, Robert Proctor, *et al*. Uplink Array Demonstration with Ground-Based Calibration [R]. JPL IPN Progress Report 42-176D, **(2009)**.
[7] Jia Liu, Xueshu Shi, *et al*. Analysis of Phase Correction Method for the Uplink Antenna Arraying based on the InSAR [J]. remote telemetry, **(2014)**, 35(6): 20-23.
[8] Wanzheng Lu. Theory and Technology of Antennas [M]. Xi'an: Xi'an University of Electronic Science and Technology Press, **(2004)**: 74-76.
[9] Zhixiong Wang, Zhonghua Fang, *et al*. Far Field of Circular Aperture [J]. Environmental Engineer of the Equipment, **(2009)**, 6(2): 82-85.
[10] Guoxi Liu, Guihai Ma, *et al*. Application of MATLAB in the Three-dimensional Pattern of Reflector Antenna [J]. Technology of the Radio communication, **(2011)**, 37(3): 36-38.
[11] Maoge Xu. Analysis on Technology of the Uplink Antenna Arraying in Deep Space Network [J]. Technology of the Telecommunications, **(2009)**, 49(6): 49-52.
[12] Xiaofeng Zhao. Data Analysis and Simulation of Electromagnetic Radiation based on MATLAB [M]. Shanghai: Fudan University, **(2008)**.
[13] Larry R. D'Addario. Combining Loss of a Transmitting Array due to Phase Errors [R]. IPN Progress Report 42-175, November 15, **(2008)**.
[14] J.I. Statman, D.S. Bagri, C.S. Yung, *et al*. Optimizing the Antenna Size for the Deep Space Network Array [R]. IPN Progress Report 42-159, **(2004)**.
[15] Chunmei Zhao, Decheng Zhang, *et al*. LEO Satellite of Precise Orbit Determination based on Spaceborne GPS/BDS [J]. Navigation Sinica, **(2015)**, 3(3): 18-23 + 34.